

<https://doi.org/10.1038/s42949-024-00159-8>

Building energy savings by green roofs and cool roofs in current and future climates

Siqi Jia^{1,2}, Qihao Weng^{1,2}✉, Cheolhee Yoo^{1,2}, Huijuan Xiao³ & Qingwei Zhong⁴

The global energy demand has greatly impacted greenhouse gas emissions and climate change. Since buildings are responsible for a large portion of global energy consumption, this study investigates the energy-saving potential of green roofs and cool roofs in reducing building energy consumption. Using an integrated approach that combines climate change modeling and building energy simulation, the study evaluates these strategies in six global cities (Cairo, Hong Kong, Seoul, London, Los Angeles, and Sao Paulo) under current and future climate change scenarios. The results show that in future climates, the implementation of green and cool roofs at the city level can lead to substantial annual energy reductions, with up to 65.51% and 71.72% reduction in HVAC consumption, respectively, by 2100. These findings can guide the implementation of these strategies in different climatic zones worldwide, informing the selection and design of suitable roof mitigation strategies for specific urban contexts.

The process of urbanization has gained momentum since the start of the 21st century, with expansive urban growth being a major contributor to higher per capita greenhouse gas emissions in urban areas^{1–3}. These emissions have been accumulating at an accelerated pace and are causing significant changes to global temperature and climate patterns^{4,5}. In urban areas, this issue may be further exacerbated by the Urban Heat Island (UHI) effect^{6,7}. A higher urban temperature has a serious impact on building energy consumption by increasing the energy and electricity necessary for cooling⁸. Over the past four decades, there has been a steady increase in building energy demand by an annual rate of 1.8%, resulting in a staggering 72% increment^{9,10}. Given the significant contribution of the built environment to higher energy demands, GHG and air pollutant emissions, human health risks and discomfort, etc., it has become increasingly crucial to develop feasible methods for reducing building energy use^{8,11,12}.

Regarding roofs, two popular strategies for reducing building energy consumption are cool roofs and green roofs^{13,14}. Cool roofs use reflective surfaces to reduce heat absorption, while green roofs use vegetation to provide insulation and reduce heat absorption. Numerous studies have shown that both green roofs and cool roofs are effective in reducing energy consumption^{15–18}, while their efficiency is significantly influenced by local climate conditions and building characteristics. However, most of those studies have only considered a few selected buildings in case studies or have focused primarily on the summer season^{13,19}, leading to a lack of research on

how variations in ambient climate and built environment influence the energy-saving potential of these technologies. Furthermore, while many studies have explored the effectiveness of green roofs and cool roofs under current climate conditions, there is a critical need for research that assesses their performance under future climate scenarios. Therefore, a comprehensive study that compares these two technologies in different climate settings under both current and future conditions is called for.

Building energy consumption is greatly susceptible to meteorological feedback, which refers to the dynamic interactions between the building and the surrounding environment, particularly local weather conditions²⁰. The heating, cooling, and ventilation requirements of a building are influenced by meteorological feedback, which can have a significant impact on energy consumption. Studies have shown that reducing outdoor air temperature by 1 °C can result in a 5% reduction in building energy consumption^{21,22}. Accurate prediction and modeling of meteorological feedback is crucial for optimizing building energy performance and reducing energy consumption. Building energy simulation models commonly use Typical Meteorological Year (TMY) weather files to represent historical and current weather conditions²³. A TMY for a given location is formed by selecting, through statistical methods, one typical meteorological month for each of the 12 calendar months from a period of years and concatenating the 12 months to form a TMY^{24,25}. However, it is important to note that TMY data is typically based on long-term historical weather data from a single

¹JC STEM Lab of Earth Observations, Department of Land Surveying and Geo-Informatics, The Hong Kong Polytechnic University, Hung Hom, Hong Kong.

²Research Centre for Artificial Intelligence in Geomatics, The Hong Kong Polytechnic University, Hung Hom, Hong Kong. ³Department of Civil and Environmental Engineering, The Hong Kong University of Science and Technology, Clear Water Bay, Kowloon, Hong Kong. ⁴The School of Nursing, The Hong Kong Polytechnic University, Hung Hom, Kowloon, Hong Kong. ✉e-mail: qihao.weng@polyu.edu.hk

weather station, which may not accurately represent the weather conditions for other locations that are far from the observed station²⁶. Therefore, additional modeling techniques are needed to incorporate ambient micro-scale climatic conditions and ensure accurate results in energy simulations.

In summary, there are three research gaps in the existing literature that have been identified. These gaps include (1) limited research on comparing the energy-saving potential of green and cool roofs by accounting for variations in ambient climate and built environment; (2) lack of studies that fully assess the impact of future climate change on green-roof and cool-roof energy-saving performance under different climate scenarios; (3) model constraints that limit detailed simulation of the effect of micro-climate on building energy use. To address these gaps, this study proposes an integrated approach to study the potential of building energy reductions by green roofs and cool roofs in different climate scenarios. This approach combines

climate change modeling and building energy simulation to quantify the effect of climate change on building energy demand. Figure 1 illustrates the development of this modeling approach.

The specific research objectives include: (1) developing the integrated modeling approach for detailed building energy simulation; (2) identifying the impacts of local ambient climate on the energy-saving performance of green roofs and cool roofs; (3) identifying the impacts of urban built environment on the performance of two roof types; and (4) predicting the energy-saving performance of two roof types under different Shared Socioeconomic Pathways (SSPs). This research has the potential to inform policy decisions on building design and energy consumption reduction strategies. The findings may also provide insights into the most effective roof-level strategies for reducing building energy consumption in different regions worldwide in the future.

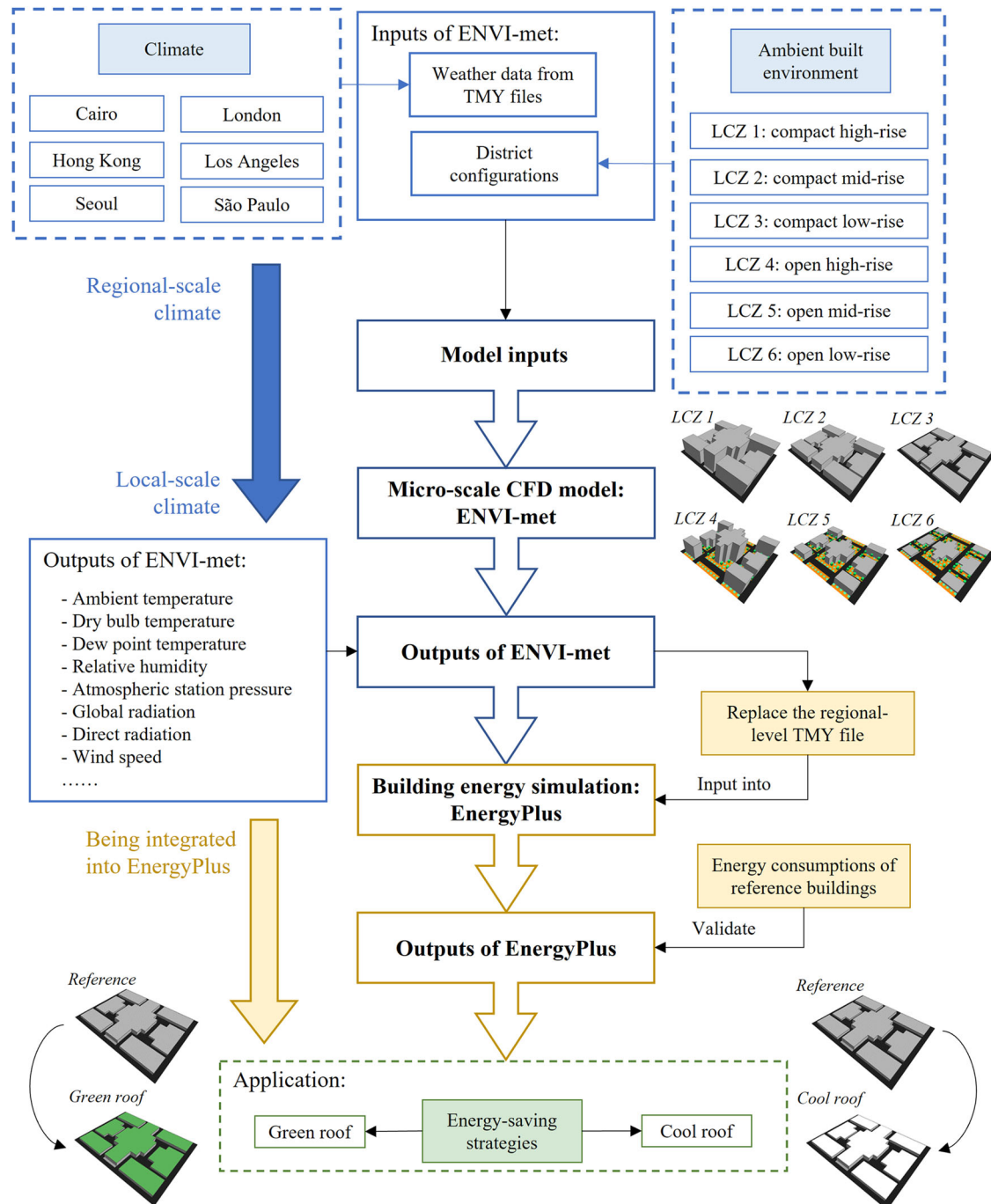


Fig. 1 | Development of the integrated modeling approach.

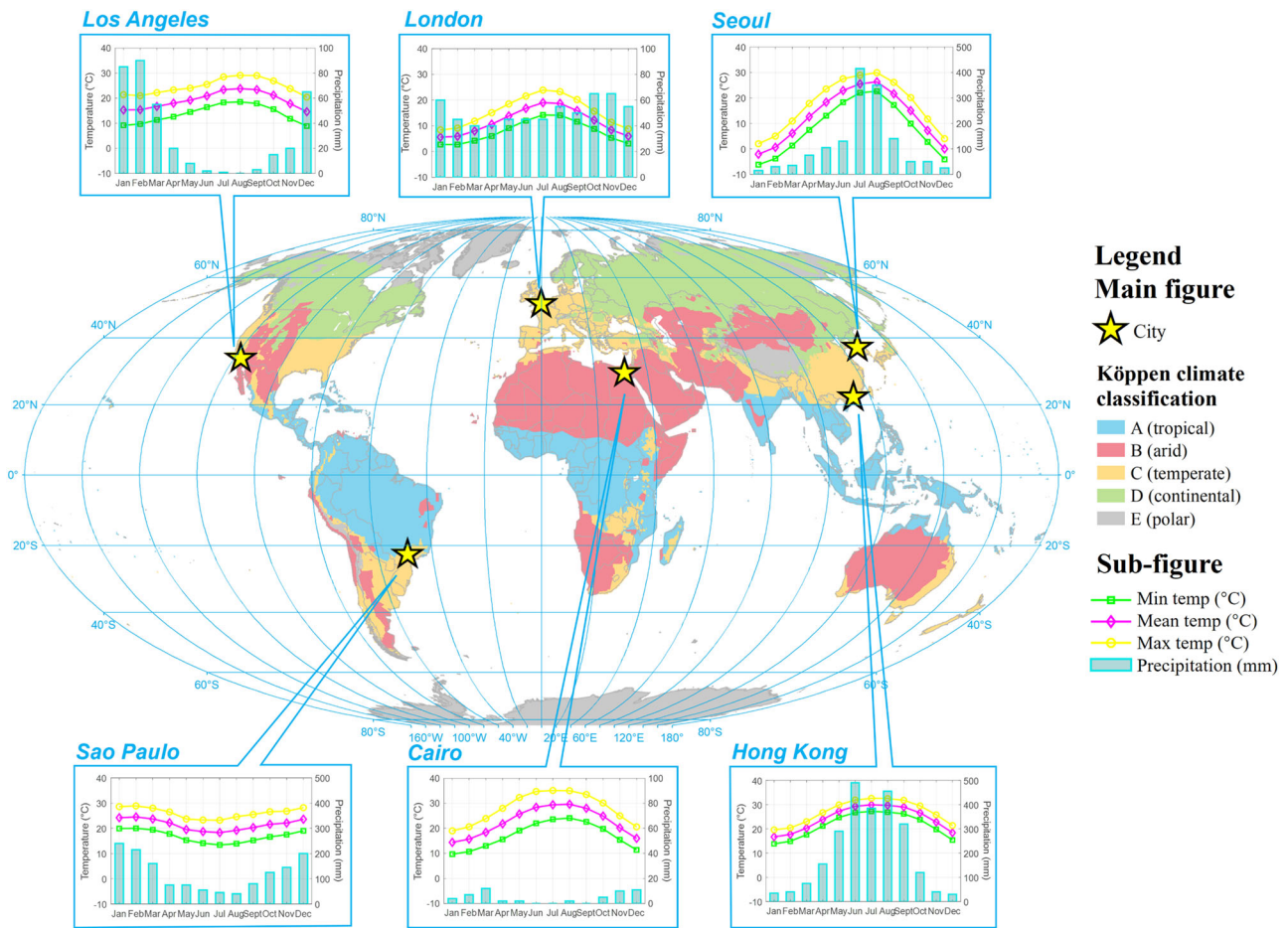


Fig. 2 | Locations and background climates of six selected cities. The Köppen-Geiger climate classification maps were obtained from ref. 27 The climatological data for each city is based on monthly averages from the 30-year period of 1981–2010. The data was sourced from the World Meteorological Organization (WMO).

Case studies were conducted in six selected cities from different climatic zones, as classified by the Köppen climate classification system²⁷, including: Cairo (Arid or desert climate; hot-dry summer and mild winter); Hong Kong (Subtropical climate; hot-humid summer and mild winter); Seoul (Temperate zone; hot-humid summer and cold-dry winter); London (Temperate oceanic climate; cool, humid and rainy weather all year round); Los Angeles (Mediterranean climate; dry summer and rainy winter, but relatively modest transitions in temperature); and São Paulo (Subtropical climate; rainy summer and dry winter, but relatively modest transitions in temperature). Figure 2 displays locations and current background climates (i.e., monthly average temperature and precipitation) of the six cities.

Results

Effect of local ambient climate on building energy savings of cool and green roofs

The proposed integrated modeling framework was used to simulate the energy use of buildings in six cities with varying local climates over a 1-year period. We compared the energy consumption of buildings installing cool roofs and green roofs to a reference building using concrete roofs without any energy-saving strategies. The comparison results are shown in Fig. 3, which displays the annual reduction of both cooling and heating energy by cool roofs and green roofs in each city.

It is found that the energy-saving performance of cool roofs and green roofs varied across different climates. Observed from Fig. 3a, the mean cooling energy reduction of cool roofs ranged from 67.18% to 86.70% among the six cities, while the mean reduction of green roofs ranged from 63.38% to 83.21%. In most study regions, the cooling energy reduction effect of cool roofs was slightly better than that of green roofs. The best cooling

energy reduction effects for cool roofs and green roofs were observed in London and Sao Paulo, respectively, with mean reduction rates of 86.7% and 87.9% across different built environments.

However, as indicated by the negative heating energy reduction rates of cool roofs in Fig. 3b, cool roofs increase building heating energy loads among all cities. Our results are in agreement with previous studies^{18,28} that the high reflectance of cool roof materials decreased heat absorption. The average increments of heating energy use for building with cool roofs can reach up to 22.5% in Sao Paulo. In contrast, the energy-saving benefits of green roofs remain steady regardless of the season. This is due to the extra insulation soil layer, which tends to keep heat stored in the buildings²⁹. Figure 3b shows that the heating energy reduction effect of green roofs was relatively significant in Sao Paulo, Cairo, and Los Angeles. Overall, the results suggest that both cool roofs and green roofs are effective for reducing cooling energy consumption in buildings across different climates worldwide, while the heating energy increments for buildings using cool roofs should be carefully considered, particularly in cities with colder climates.

Effect of urban built environment on building energy savings of cool and green roofs

In this study, the effect of the urban built environment, characterized by local climate zones (LCZs), on building energy savings by cool roofs and green roofs was analyzed. A LCZ is defined as a region of uniform surface cover, structure, material, and human activity³⁰. These zones, which are localized, climatically-driven, and representative of specific areas, are designed to describe landscapes with distinct thermal climates based on their surface properties³¹. LCZs are being used in numerous studies focusing on temperature, ecological, and other environmental variables^{32–35}.

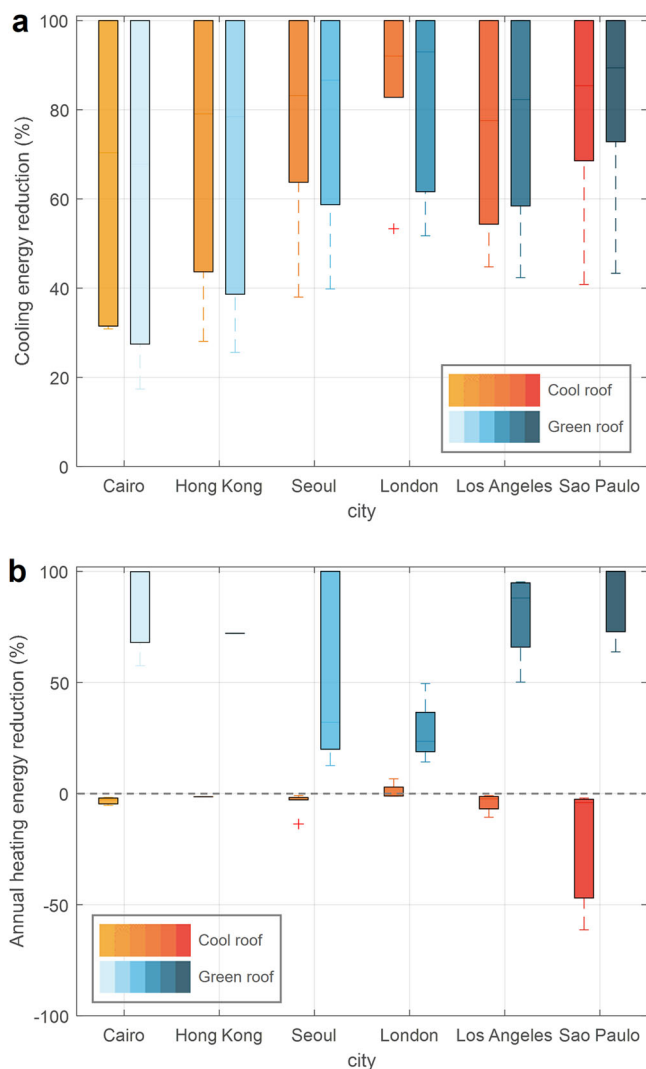


Fig. 3 | Effect of local ambient climate on building energy savings of cool and green roofs. Annual building energy reduction by cool and green roofs in different climates among cities: (a) annual cooling energy reduction by two roofs in each of six selected cities; and (b) annual heating energy reduction by two roofs in each of six selected cities.

The simulation was conducted for each LCZ among all the cities. The annual energy reduction ranges for both cooling and heating energy by two roof types in different built environments were identified. Figure 4 shows the comparison results of the annual energy reduction effects by cool roofs and green roofs in each LCZ.

The results indicate that the urban built environment plays a crucial role in determining the energy-saving effects of both cool roofs and green roofs. Figure 4a shows significant variations in cooling energy reductions by both types of roofs in different LCZs, with mean reduction rate ranging from 39.30% to 100% for cool roofs and 38.38% to 100% for green roofs. Notably, LCZs 3 and 6, characterized by low-rise buildings, can achieve nearly zero annual energy demands for cooling by installing either cool roofs or green roofs. In addition, the cooling energy reduction effect of both types of roofs decreased with increasing building height. The least cooling energy reduction effect was observed in LCZ 4 (i.e., open high-rise built environment), with mean cooling energy reduction rate of 39.3% and 38.4% for buildings using cool roofs and green roofs, respectively. Figure 4b shows that the building heating energy-saving performance of green roofs ranged from 47.4% to 100% across LCZs and decreased with increasing building height. However, the relationship between the built environment and the heating

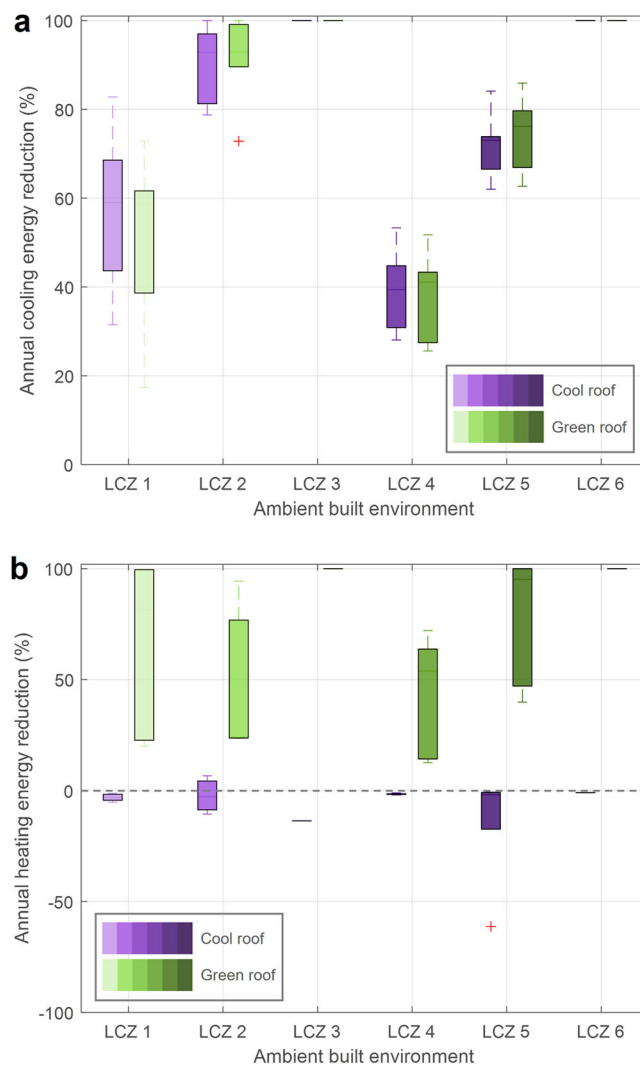


Fig. 4 | Effect of urban built environment on building energy savings of cool and green roofs. Annual building energy reduction by cool roofs and green roofs among different LCZs: (a) annual cooling energy reduction by two roofs in LCZs; and (b) annual heating energy reduction by two roofs in LCZs.

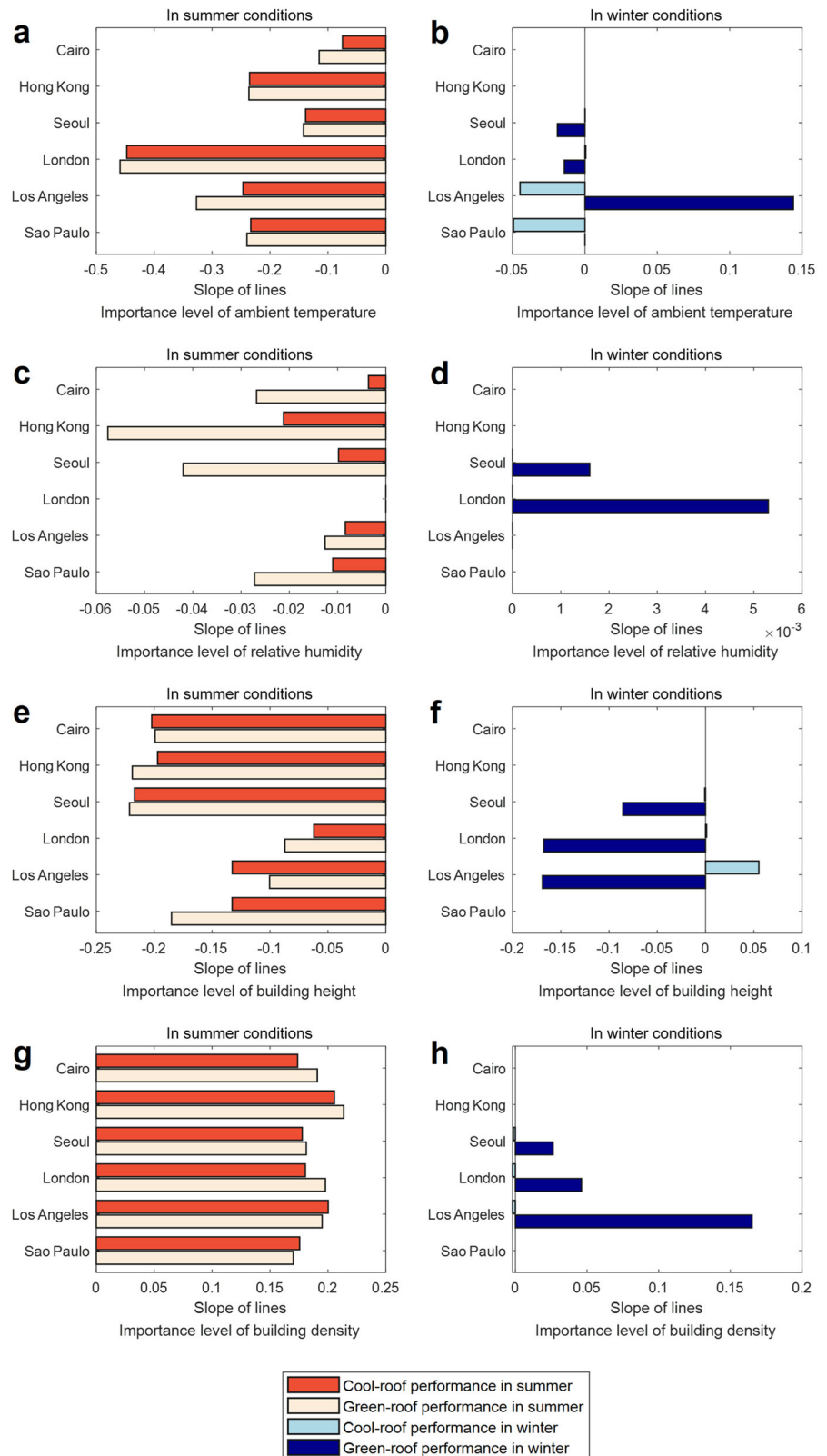
energy reduction effect of cool roofs is not straightforward. In LCZ 3, the heating energy increment caused by cool roofs was the highest at 13.7%.

Sensitivity analysis of the impacts of climate and built environment

A sensitivity analysis was performed to investigate the effect of both ambient climate and urban built environment on building energy savings of the two roof systems. The sensitivity analysis of the influence of the local climate simulated the energy-saving performance of cool roofs and green roofs under local climatic conditions characterized by different ambient temperatures and relative humidity, while for the analysis of the influences of the urban built environment, building density and height are two key parameters that affect building energy use.

In each city, a total of ten scenarios were simulated for the sensitivity analysis of each selected parameter: two baseline conditions (typical summer and winter conditions), -50%, -25%, 25%, and 50% from each baseline condition. The baseline condition for the urban layout was fixed among different cities, with building density of 50% and a building height of 40 m. The baseline summer and winter conditions in each city were derived from TMY files, with the days with the maximum and minimum daily ambient temperatures selected as the summer and winter conditions for each city, respectively. The results of simulations are shown in Fig. 5.

Fig. 5 | Sensitivity analysis of the impacts of climate and built environment. The importance level of climate and built environment on building energy savings of cool and green roofs in different conditions: **(a)** importance level of ambient temperature to energy savings on typical summer condition; **(b)** importance level of ambient temperature to energy savings on typical winter condition; **(c)** importance level of relative humidity to energy savings on typical summer condition; **(d)** importance level of relative humidity to energy savings on typical winter condition; **(e)** importance level of building height to energy savings on typical summer condition; **(f)** importance level of building height to energy savings on typical winter condition; **(g)** importance level of building density to energy savings on typical summer condition; and **(h)** importance level of building density to energy savings on typical winter condition.



The sensitivity analysis demonstrated that green roofs exhibit higher sensitivity to variations in both ambient climate and built environment compared to cool roofs. Notably, the energy-saving performance of both roof systems was found to be most influenced by changes in ambient temperature during the summer (Fig. 5a). Conversely, variations in relative humidity had the least impact on the energy-saving performance of both roof systems (Fig. 5c).

In the summer condition of London, the cool-roof curve has a slope of -0.447 , while the green-roof curve has a slope of -0.459 . This indicates a high sensitivity of building energy reduction to temperature variations. However, in winter, the energy savings provided by both roof systems become less sensitive to variations in ambient temperature. In Los Angeles, a moderate improvement in energy savings by green roofs was observed with rising air temperature (slope = 0.144 ; Fig. 5b), which can be attributed to its

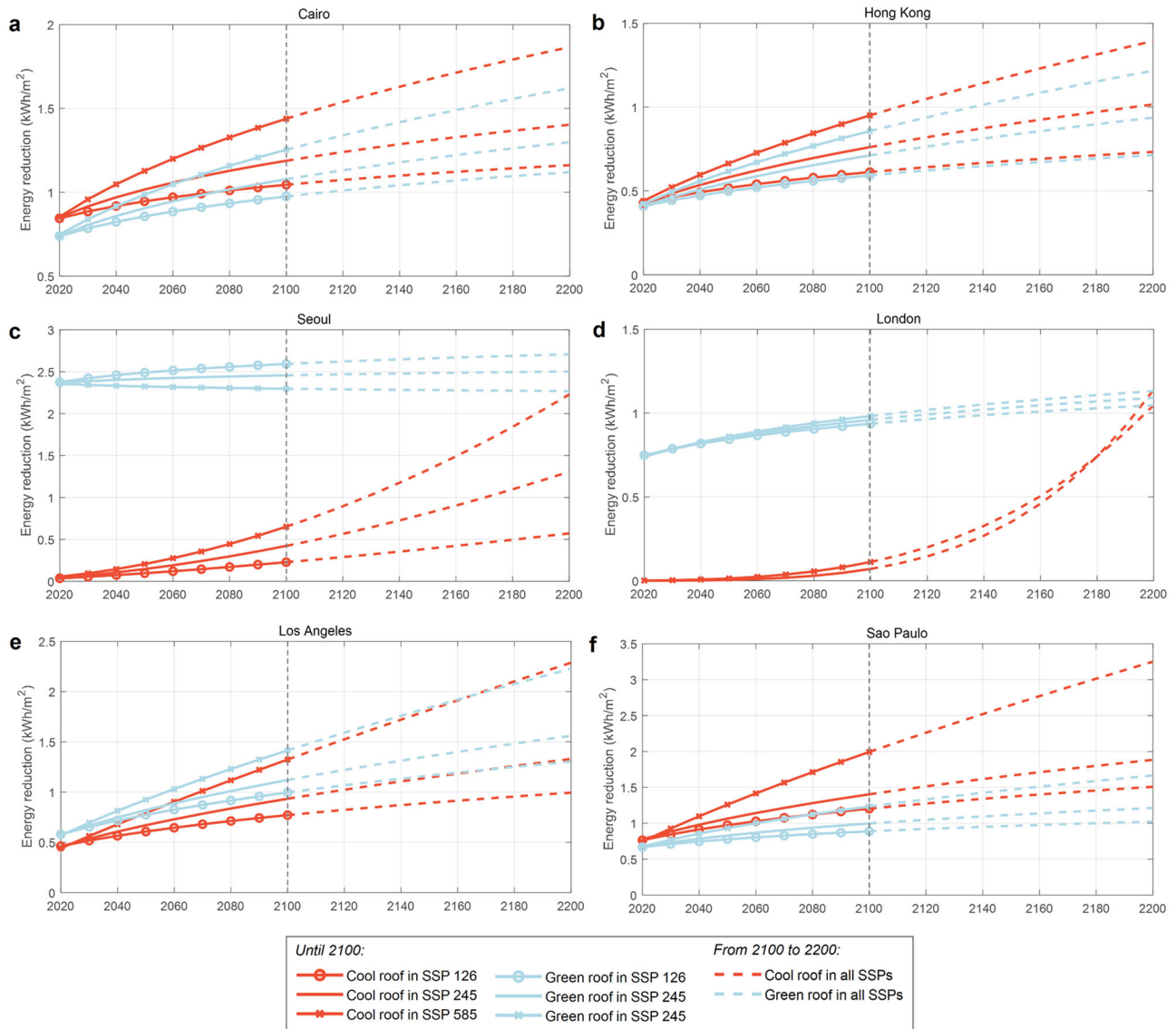


Fig. 6 | Building energy savings by cool and green roofs under different future scenarios. Future building energy-saving performance of cool roofs and green roofs under three SSP scenarios across six cities: **(a)** future building energy savings by two roofs in Cairo; **(b)** future building energy savings by two roofs in Hong Kong; **(c)** future building energy savings by two roofs in Seoul; **(d)** future building energy savings by two roofs in London; **(e)** future building energy savings by two roofs in Los Angeles; and **(f)** future building energy savings by two roofs in Sao Paulo.

building energy savings by two roofs in Seoul; **d** future building energy savings by two roofs in London; **e** future building energy savings by two roofs in Los Angeles; and **(f)** future building energy savings by two roofs in Sao Paulo.

Mediterranean climate. In such climates, the low plant evaporation and transpiration rates reduce heat loss through vegetation, allowing more heat to be stored inside buildings through the insulation soil layer. Compared to the remarkable effect of ambient temperature on building energy reduction by the two roof systems, humidity has minimal influence on the energy-saving capabilities of cool roofs (Fig. 5c, d). Similarly, the sensitivity of energy savings by green roofs to variations in relative humidity is generally limited.

Regarding the effect of building arrangement (Fig. 5e–h), consistent patterns of decreasing and increasing energy savings were observed for both cool roofs and green roofs with increasing building heights and building densities, respectively. In summer, the sensitivity of energy reduction effects by both roof systems to variations in the built environment is similar. The slope of the line ranges from -0.217 to -0.062 for cool roofs and from -0.221 to -0.087 for green roofs, corresponding to varying building height ranges. The slope of the line for both roof systems in relation to varying building densities ranges from 0.174 to 0.206 and 0.170 to 0.214 , respectively. In winter, the difference in the sensitivity of energy-saving effects between the two roof systems can be more significant. The energy reduction

provided by green roofs was found to be more sensitive to variations in the built environment compared to cool roofs. The most substantial impact of the built environment on energy savings by both roof systems was observed in Los Angeles.

Energy savings in buildings by green roofs and cool roofs under current and future climate scenarios

Given the limited influence of humidity on the energy-saving effect of the two strategies, only temperature variations were considered in the sensitivity analysis for three SSP scenarios (SSP 1–2.6, SSP 2–4.5, and SSP 5–8.5) from 2021 to 2100. Hourly temperatures were estimated using Eqs. (1–3), which utilized the current TMY weather files of each city and the future projected values averaged from six selected Global Climate Models, namely HadGEM3 GC31-LL, MIROC6, MRI-ESM2-0, CMCC-ESM2, ACCESS-CM2, and BCC-CSM2-MR. The future energy-saving potentials of cool roofs and green roofs were then explored under these three SSPs. Based on the relationship between the energy-saving of the two roof systems and climate projections until 2100, future trends of energy-saving performance were projected until 2200. Figure 6 shows the performance of the two roof

systems in building energy reduction across six cities under future climate scenarios.

The results demonstrate that the effectiveness of cool roofs and green roofs in reducing building energy use varies with climatic zones and future climate change scenarios. With the anticipated global temperature increase in the future, the global energy demand for air conditioning is expected to rise. Simultaneously, the energy savings provided by both cool roofs and green roofs are also projected to increase. The energy-saving effect of both roofs is generally more pronounced in scenarios characterized by a significant warming trend (i.e., SSP 5–8.5). Under most future conditions, cool roofs tend to have a more substantial energy reduction effect compared to green roofs. Figure 6f shows that cool roofs can achieve the highest building energy savings in Sao Paulo, ranging from 1.09 kWh/m² to 1.91 kWh/m² under three SSPs by 2100, which correspond to 37.22% to 65.52% of the total HVAC energy consumption. This can be explained by the significant global warming trend expected in the next few decades.

On average, Global Climate Models project global mean temperature increases of around 1 °C, 2 °C, and 4 °C from 2021 to 2100 under SSPs 1–2.6, 2–4.5, and 5–8.5, respectively. However, certain cities may experience even higher temperature increases than the global average. For example, Sao Paulo is projected to witness average temperature increases of up to 1.12 °C, 2.54 °C, and 5.50 °C by 2100 under these three SSPs.

In cities situated in warm climatic zones like Cairo, Hong Kong, Los Angeles, and Sao Paulo, cool roofs generally outperform green roofs in terms of cooling energy reduction under the same SSP scenarios, except for Los Angeles where green roofs show better energy-saving performance in future climates (Fig. 6e). Notably, the energy savings by green roofs in Sao Paulo can reach 71.72% of the total HVAC consumption by 2100 under SSP 5–8.5. In colder cities, such as Seoul and London, where the energy demand for heating is high, green roofs may offer greater energy savings than cool roofs due to their insulation effect, which helps to keep the indoor environment warm. Consequently, it is advisable to prioritize the implementation of green roofs in these cities in the future. This contrast in energy-saving performance between the two roof systems is also evident in Fig. 6c, d. In the future climates in Seoul, green roofs can save the most energy at over 2 kWh/m² (around 30% of the total HVAC energy use) under both current and future climate scenarios. However, with the increasing global warming, the demand for heating is expected to decrease. As a result, a significant upward trend in energy reduction by cool roofs can be observed in the future climates of London and Seoul, particularly from 2100 to 2200.

Discussion

Cool roofs and green roofs are two energy-efficient strategies that have the significant potential to reduce building energy consumption and contribute to climate change mitigation efforts. However, their effectiveness can vary depending on the specific built environment and climate conditions. Therefore, it is important to carefully assess their performance in different scenarios. This research evaluates the potential of cool roofs and green roofs for building energy reductions in different LCZs across six global cities under current and future climate scenarios. The discussion section mainly focuses on the projection of the energy-saving effectiveness of cool roofs and green roofs and their potential applications in the future.

The findings indicate that green roofs are more sensitive to variations in outdoor environmental conditions compared to cool roofs, as shown in Fig. 5. This is because the performance of green roofs depends on the growth and health of plants on the rooftops, which can be influenced by environmental factors such as temperature, precipitation, and sunlight. In contrast, the energy-saving effectiveness of cool roofs is less affected by environmental variations as they primarily rely on the reflective properties of the roof surfaces. Therefore, in regions with warm climates and cloudy or rainy conditions, where the cooling effect of greenery is limited due to reduced evaporation and transpiration rates, the use of cool roofs may be more suitable for reducing cooling energy consumption in buildings. Meanwhile, in hot and sunny regions, both cool roofs and green roofs reliably reduce energy demands throughout the year. However, in relatively cold regions,

only green roofs are effective for reducing heating energy use for buildings. These findings align with existing literature^{13,29,36,37}.

In addition, it is important to consider the urban built environment as it can significantly impact the performance of both cool roofs and green roofs. The potential overshadowing effects of adjacent buildings should be carefully evaluated and modeled. Some studies also recommend conducting solar simulation before implementing these mitigation strategies to ensure their effectiveness³⁸.

The study projects that green roofs have significant potential for application in cities with rapidly increasing temperatures and consistently low precipitation, such as Los Angeles (Fig. 6e). These cities are characterized by a humid subtropical climate with hot and humid summers and mild winters. Similarly, relatively colder cities with moderate cooling and heating demands, like Seoul with its temperate climate and distinct hot and cold seasons, can also benefit from green roofs. In tropical regions and some subtropical regions characterized by high temperature and intense solar radiation (e.g., Cairo, Hong Kong, and Sao Paulo, see Fig. 6a, b, f), cool roofs are found to be more effective in reducing future building energy use. However, it is important to consider water scarcity in urban regions, as irrigation may be necessary for green roofs in such areas³⁹. A study identified that green roofs were almost dry in desert climates like Cairo, thus most of the peculiarities of green roofs did not work²⁹. In addition, as shown in Fig. 6c, d, there is a dramatic rise in the building energy reduction performance of cool roofs in future climates of London and Seoul from 2100 to 2200, indicating the broader potential application of cool roofs as global warming trends continue.

This study provides valuable guidance for implementing cool roofs and green roofs worldwide to achieve building energy savings in the future, considering the incorporation of climate change. Previous studies often focused on the current applications of these solutions and did not consider their future implications in relation to climate change^{13,29}. Figure 7 presents the global suitability for the implementation of cool roofs and green roofs for building energy savings.

When considering the implementation of cool roofs and green roofs in building development, it is important to consider not only their energy-saving effectiveness but also their economic and environmental benefits. Cool roofs are a cost-effective option for installation and maintenance, while green roofs offer additional benefits such as reducing UHI effects, improving air quality, managing stormwater, and enhancing the durability of roofs^{38,40,41}. In highly urbanized areas, green roofs can bring even more benefits, including the enhancement of urban landscape and the well-being of residents. Therefore, the decision between cool roofs and green roofs also should be based on a comprehensive assessment of project goals, local conditions, and priorities.

In summary, this study evaluated the energy-saving performance of green roofs and cool roofs in diverse ambient climates and urban built environments. It considered both current and future climate change scenarios in six global cities: Cairo, Hong Kong, Seoul, London, Los Angeles, and Sao Paulo. To improve modeling accuracy, an integrated approach was developed, combining climate change modeling and building energy simulation.

The key findings of this research are as follows:

- The integrated modeling framework provides more precise estimations of both hourly and monthly building energy use compared to traditional modeling methods.
- The energy-saving effects of cool roofs and green roofs largely depend on the climate zones in which they are implemented. Both roof systems demonstrate significant potential in reducing cooling energy demand across various climates, while the increase in heating energy demand associated with cool roofs should be considered in cities with colder climates.
- The energy-saving effects of cool roofs and green roofs are influenced by the urban built environment. The best energy-saving performance is observed in low-rise buildings, and as building height increases, there is a decreasing trend in energy-saving performance.

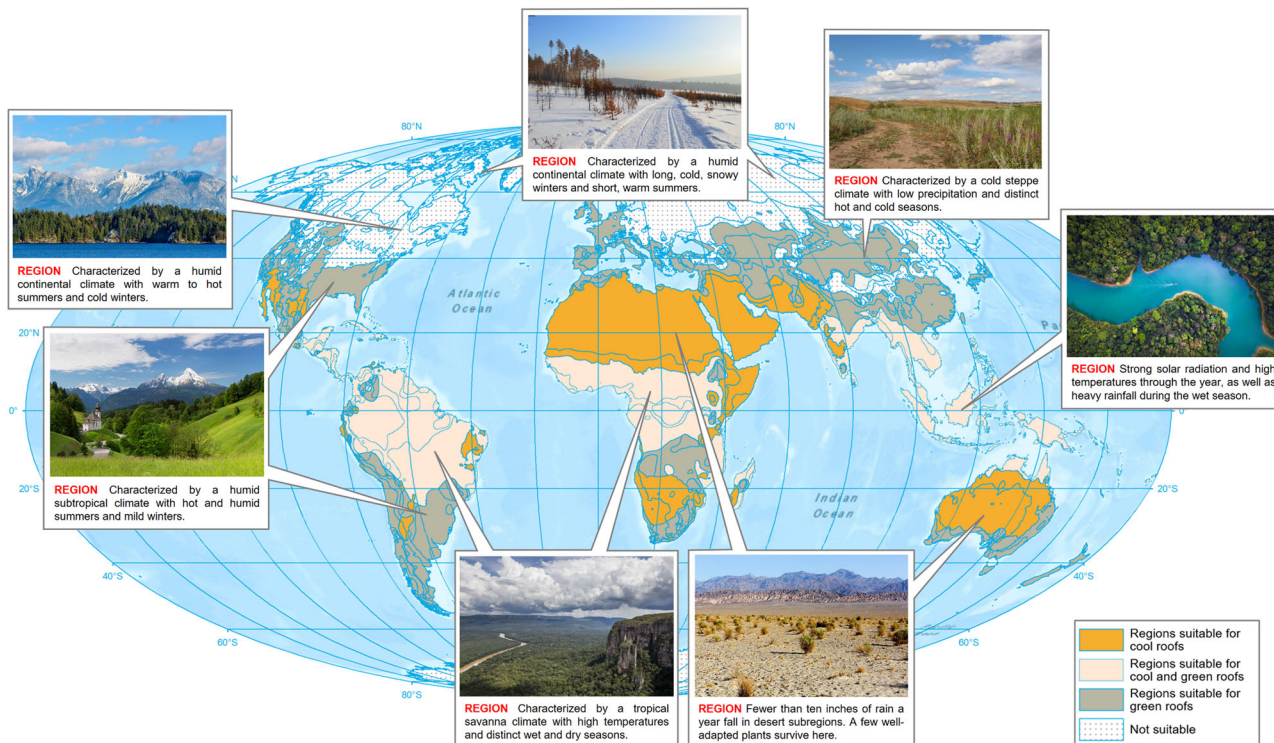


Fig. 7 | Global suitability for the implementation of cool roofs and green roofs for building energy savings.

- In future scenarios with high greenhouse gas emissions (SSP 5–8.5), cool roofs and green roofs are expected to save more cooling energy for buildings. The effects of global warming on reducing building heating energy demand should be considered in future climate projections.

This study provides valuable insights into how the energy-saving effectiveness of cool roofs and green roofs can be influenced by the specific characteristics of the local ambient climate and urban context. This information can be used to inform the selection and design of appropriate roof mitigation strategies in different urban areas, helping them adapt to and mitigate the impact of future climate change.

Methods

Current and future weather data collection

The current weather data for each city was generated using TMY weather files, which provide a reliable estimate of the typical weather patterns in a given area. TMYs contain hourly values of solar radiation and meteorological elements for a 1-year period derived from multiple years (at least 10 years)⁴². For this study, TMY datasets covering the period from 2007 to 2021 were utilized to represent the current weather information from six cities⁴³. Table 1 displays the specific locations for the TMY data in each city.

To forecast future weather conditions, one typically relies on a Global Climate Model to generate data²⁴. This model simulates Earth’s climate for future decades, typically until 2100, considering different carbon emission scenarios based on socioeconomic assumptions outlined by the IPCC. Various groups of Global Climate Models with different grid resolutions and periods are available^{44,45}. Some examples include BCCR: BCM2 (Norway), MIROC3.2 (Japan), CSIRO:MK3 (Australia), INM: CM3 and INM: CM4 (Russia), NASA: GISSAOM (USA), and BCC-CM1 (China). In this study, we adopted a total of six high-resolution Global Climate Models, namely HadGEM3 GC31-LL⁴⁶, MIROC6⁴⁷, MRI-ESM2-0⁴⁸, CMCC-ESM2⁴⁹, ACCESS-CM2⁵⁰, and BCC-CSM2-MR⁵¹. All employed models have been used widely in climate research^{24,52}. The horizontal resolutions of the employed models range from 0.9° latitude by 1.25° longitude to 1.25°

Table 1 | Detailed information for the TMY data in each city

City	Weather station No. for the TMY data	Detailed Location
Cairo	623,660	Heliopolis district (<i>residential and commercial mixed-use area</i>)
Hong Kong	450,070	Mongkok district (<i>residential and commercial mixed-use area</i>)
Seoul	471,080	Seodaemun-gu District (<i>downtown</i>)
London	037,700	St James’s district (<i>downtown</i>)
Los Angeles	722,874	University Park district (<i>Downtown</i>)
Sao Paulo	869,100	Santana district (<i>residential and commercial mixed-use area</i>)

latitude by 1.875° longitude. With relatively high resolutions, it allows for more detailed simulations of climate processes.

As defined in the IPCC Sixth Assessment Report on climate change⁵³, three Shared Socioeconomic Pathways (SSPs) scenarios were utilized in this study. SSPs represent climate change scenarios that consider projected global socioeconomic changes^{54,55}. These three SSPs are SSP 1–2.6 (low carbon scenario), SSP 2–4.5 (intermediate carbon scenario), and SSP 5–8.5 (very high carbon scenario). These scenarios provide insights into potential future climate conditions under different levels of carbon emissions.

Designs of green roof and cool roof

Three roof designs were included. In the optimized scenarios where green or cool roofs are implemented, it is assumed that all buildings within the LCZ are installed with green roofs or cool roofs. The control simulation was run using a roof albedo of 0.2 as the baseline case, with no green roofs or cool roofs.

The green roof design used in this study was chosen based on specific parameters that are known to significantly impact roof performance in terms of heat absorption and energy savings. A sensitivity analysis conducted by ref. 56 identified four parameters with a strong influence: (1) the

height of plants (h); (2) the leaf area index (LAI), which is defined as the ratio of the projected leaf area to the overall ground area; (3) the minimum stomatal resistance (m_{sr}); and (4) the dry soil conductivity (k). According to the literature^{13,56}, typical values for these parameters were used: $h = 0.50$ m; $LAI = 2$; $m_{sr} = 180$ s/m; $k = 0.33$ W/mK⁻¹, with a growing medium depth of 0.20 m. It is important to clarify that this research does not incorporate variations of these parameters with time, as it focuses solely on simulating their performance in cooling and energy savings under specific conditions, rather than modeling their long-term time-series performance. The soil layer is comprised of sandy loam and Styrofoam, with respective depths of 1.333 m (2/3 of the total depth) and 0.067 m (1/3 of the total depth).

The primary technical factors influencing the performance of a cool roof are the solar reflectance and thermal emissivity¹³. In the present study, a typical design of cool roof was employed¹³, which featured a light-colored coating with a solar reflectance (r) of 0.80 and a thermal emissivity (ϵ) of 0.90. Other parameters and designs of different roof systems used in this study can be found in Supplementary Note 1.

Building energy data for validation

The Building Data Genome 2 Dataset is an open dataset that consists of 3053 energy meters from 1636 buildings⁵⁷. The dataset includes time-series data spanning two continuous years (2016–2017) at an hourly frequency. These meters were collected from 19 sites located in the North America and Europe. A random selection of 10 buildings was made from the database for validation. These buildings were situated in 9 cities across North America and Europe, representing 6 diverse ASHRAE Climate Zones. The selected buildings encompassed various primary use categories such as residential, education, industrial, office, and healthcare. More detailed information about the validation dataset can be found in Supplementary Note 2.

Downscaling of global climate models

Global Climate Models are numerical computer-driven models that simulate the physical processes in the Earth’s atmosphere and oceans. They predict future climate conditions at a coarse spatial resolution, which makes them unsuitable for direct use in building energy simulation⁵⁸. To address this limitation, a process known as downscaling is required to convert the model output to suitable temporal and spatial resolutions⁴⁴. In this study, a downscaling method proposed by ref. 59 is adopted. This method involves adjusting present-day design weather data based on the projected changes in climate forecasted by Global Climate Models and regional climate models. The downscaling process utilizes time series analysis techniques to derive future hourly weather data at a finer resolution for the six study cities. By employing this downscaling methodology, the future climate data for the study cities can be obtained at hourly resolution, enabling more accurate building energy simulations.

The method used in this study, referred to as “morphing”⁵⁹, involves shifting and stretching the climatic variables in the present-day weather time series to generate weather time series that encapsulate the average climate change. This process aims to maintain the realistic weather patterns of the original data while incorporating the projected climate changes. To be more specific, the method consists of three steps: (i) shifting (Eq. (1)); (ii) linear stretch (Eq. (2)); and (iii) the combination of the previous two steps (Eq. (3)). The equations for these steps are as follows:

$$x = x_0 + \Delta x_m \tag{1}$$

$$x = \alpha_m x_0 \tag{2}$$

$$x = x_0 + \Delta x_m + \alpha_m (x_0 - (x_0)_m) \tag{3}$$

where x_0 is an existing hourly climatic variable, derived from current TMY weather files, Δx_m is the absolute change in the monthly-mean climatic variable for month m , α_m is the fractional change in the monthly-mean climatic variable for month m and $(x_0)_m$ is the climatic variable x_0 averaged over month m . By using this method, the future TMY weather data can be

constructed using existing TMY weather data files and predicted climate change.

Future climate projections

After applying the morphing method to the current TMY data, the projection results of future climate data in the year 2100 are calculated. Table 2 shows the annual average value of key climatic variables (i.e., dry-bulb temperature (°C) and precipitation (mm)) for the six cities under these three SSPs: SSP 1–2.6, SSP 2–4.5, and SSP 5–8.5 in 2100. A common approach to select global models to use in the regional studies is to average over all employed models⁷². In this study, the future climate averaged from the six selected Global Climate Models in different SPPs was used.

Development of the integrated modeling approach

This research proposes an integrated modeling approach that combines a micro-level Computational Fluid Dynamics (CFD) model (i.e., ENVI-met 5.1.1) and a building energy simulation program (i.e., EnergyPlus 9.6).

EnergyPlus is an open-source simulation program used for estimating building energy use, including heating, cooling, ventilation, and lighting⁶⁰. It allows users to model buildings with integrated thermal controls and mechanical and electrical systems, facilitating simulations based on actual building descriptions⁶¹. Traditionally, EnergyPlus simulates building energy usage by incorporating regional weather information (EnergyPlus Weather files) and building information. However, in this integrated approach, we have coupled ENVI-met with EnergyPlus for building energy simulation. ENVI-met is a CFD model renowned for accurately simulating atmospheric flow and heat transfer in complex urban geometries. As a widely utilized tool for studying urban atmospheric processes^{62,63}, its detailed representation of atmospheric processes makes it effective for simulating climate change impacts and evaluating urban adaptation strategies⁶⁴. The forcing weather data required for the ENVI-met simulations was obtained from EnergyPlus Weather (EPW) files for each of six evaluated cities, while the model domain was described by the LCZ classification system³⁰. By incorporating localized meteorological outputs from ENVI-met to modify the TMY weather inputs, we anticipate achieving higher accuracy in estimating building energy usage.

The integrated modeling framework described in this research provides a robust tool for conducting comprehensive observations and simulations of local physical environments and meteorological conditions. Following a validation process, this approach, which incorporates micro-scale meteorological parameters, has shown to provide more precise estimations of building energy usage compared to traditional modeling methods that rely on regional weather files as model inputs. A thorough validation process and the corresponding results can be found in Supplementary Note 3.

Scenario development

To accurately model the local climatic effects of implementing cool roofs and green roofs at the city level, the concept of local climate zone (LCZ) was utilized. The global LCZ map of 100 m-resolution, generated by ref. 65, was used in this study. Six urban layouts were constructed according to the specifications of the built-up LCZs^{30,66}, including: (1) LCZ 1: compact high-rise environment; (2) LCZ 2: compact mid-rise environment; (3) LCZ 3: compact low-rise environment; (4) LCZ 4: open high-rise environment; (5) LCZ 5: open mid-rise environment; and (6) LCZ 6, open low-rise environment. The computational domain for each LCZ in ENVI-met was set as $X \times Y = 200$ m \times 225 m, with grid cells of 5 m. Initial methodological conditions are specified in TMY of each city. The internal load settings for buildings were based on the prototype building models developed by the U.S. Department of Energy (DOE). After running LCZ-based simulations for each city, we multiplied the energy-saving potentials for individual LCZs by the percentage of each LCZ’s coverage in the cities, as obtained from the global LCZ map⁶⁵.

The designs of each urban LCZ were based on the LCZ definitions proposed by ref. 30. For compact urban layouts (LCZs 1–3), buildings occupy 60% of the total area in the modeled domain, while in open layouts

Table 2 | Annual average values of key climatic variables among the six cities in 2100

(a) SSP 1–2.6						
	HadGEM3 GC31-LL	MIROC6	MRI-ESM2-0	CMCC-ESM2	ACCESS-CM2	BCC-CSM2-MR
(a) Cairo						
Temperature (°C)	14.84	13.81	13.45	15.06	14.68	13.63
Precipitation (mm)	5.70	5.70	5.70	5.70	5.70	5.97
(b) Hong Kong						
Temperature (°C)	18.05	15.75	16.00	16.97	17.38	16.20
Precipitation (mm)	31.38	31.66	33.63	35.05	36.54	39.27
(c) Seoul						
Temperature (°C)	−0.20	−1.78	−1.52	0.15	−0.64	−1.15
Precipitation (mm)	23.38	21.53	24.84	23.29	22.82	27.00
(d) London						
Temperature (°C)	6.05	4.32	3.86	6.58	6.47	5.62
Precipitation (mm)	70.16	64.46	72.12	72.61	68.18	88.13
(e) Los Angeles						
Temperature (°C)	11.98	11.05	10.72	11.71	11.69	11.23
Precipitation (mm)	133.70	78.01	83.95	82.93	79.66	117.68
(f) São Paulo						
Temperature (°C)	26.24	24.86	24.81	25.08	25.91	24.97
Precipitation (mm)	223.07	218.61	226.47	266.95	230.74	346.11
(b) SSP 2–4.5						
	HadGEM3 GC31-LL	MIROC6	MRI-ESM2-0	CMCC-ESM2	ACCESS-CM2	BCC-CSM2-MR
(a) Cairo						
Temperature (°C)	15.56	14.69	14.60	15.99	15.80	15.48
Precipitation (mm)	5.81	5.80	5.78	5.63	5.88	5.74
(b) Hong Kong						
Temperature (°C)	18.82	16.40	16.26	17.48	18.14	17.12
Precipitation (mm)	39.95	31.48	29.55	31.63	35.04	33.48
(c) Seoul						
Temperature (°C)	1.28	−0.36	−0.82	1.40	0.53	0.72
Precipitation (mm)	25.12	22.78	22.29	24.46	24.83	24.35
(d) London						
Temperature (°C)	7.48	4.89	4.48	6.70	7.15	6.03
Precipitation (mm)	70.29	62.80	80.82	70.32	68.00	94.69
(e) Los Angeles						
Temperature (°C)	13.26	11.99	11.50	12.66	12.32	12.19
Precipitation (mm)	98.15	82.26	84.55	79.67	86.80	117.93
(f) São Paulo						
Temperature (°C)	27.29	25.62	25.53	25.77	26.96	25.65
Precipitation (mm)	257.84	222.68	229.97	268.68	237.10	352.61
(c) SSP 5–8.5						
	HadGEM3 GC31-LL	MIROC6	MRI-ESM2-0	CMCC-ESM2	ACCESS-CM2	BCC-CSM2-MR
(a) Cairo						
Temperature (°C)	18.33	16.73	16.35	17.53	18.03	16.60
Precipitation (mm)	6.52	5.84	5.78	6.28	6.43	6.49
(b) Hong Kong						
Temperature (°C)	21.54	18.08	18.00	18.95	20.73	18.02
Precipitation (mm)	28.71	30.04	28.55	24.95	32.59	37.61
(c) Seoul						
Temperature (°C)	3.90	2.73	2.12	3.02	3.30	1.62
Precipitation (mm)	27.09	23.50	26.87	24.68	27.93	24.97

Table 2 (continued) | Annual average values of key climatic variables among the six cities in 2100

(c) SSP 5-8.5						
	HadGEM3 GC31-LL	MIROC6	MRI-ESM2-0	CMCC-ESM2	ACCESS-CM2	BCC-CSM2-MR
(d) London						
Temperature (°C)	9.16	6.35	6.06	7.80	8.84	6.95
Precipitation (mm)	79.70	64.87	80.44	82.68	74.44	106.63
(e) Los Angeles						
Temperature (°C)	15.40	13.78	13.37	13.84	14.51	13.70
Precipitation (mm)	140.38	84.89	87.94	117.45	92.22	143.14
(f) São Paulo						
Temperature (°C)	30.15	27.21	27.02	27.35	29.65	27.77
Precipitation (mm)	276.20	221.14	223.38	280.67	267.42	393.04

Table 3 | Geometric and surface cover properties for each LCZ

LCZ	Description	Sky view factor	Aspect ratio	Building surface fraction (%)	Impervious surface fraction (%)	Pervious surface fraction (%)	Height (m) of roughness elements
LCZ 1	Compact high-rise	0.2–0.4	>2	40–60	40–60	<10	>35
LCZ 2	Compact mid-rise	0.3–0.6	0.75–2	40–70	30–50	<20	10–25
LCZ 3	Compact low-rise	0.2–0.6	0.75–1.5	40–70	20–50	<30	3–10
LCZ 4	Open high-rise	0.5–0.7	0.75–1.25	20–40	30–40	30–40	>25
LCZ 5	Open mid-rise	0.5–0.8	0.3–0.75	20–40	30–50	20–40	10–25
LCZ 6	Open low-rise	0.6–0.9	0.3–0.75	20–40	20–50	30–60	3–10

(LCZs 4–6), buildings occupy 30%. The building heights in high-rise, mid-rise, and low-rise configurations are 30–60 m (around 10–20 story height), 15–24 m (around 5–8 story height), and 3–9 m (around 1–3 story height), respectively. For LCZs 1–3, the surfaces consist of concrete and asphalt pavement with default albedos of 0.5 and 0.2, respectively. In LCZs 4–6, except concrete and asphalt pavement, a loamy soil surface with an albedo of 0 and emissivity of 0.9 is utilized. Different types of vegetation are distributed on the soil surface uniformly, including grass (height: 0.25–0.5 m, leaf area density: 0.3) and trees (height: 2–10 m, leaf area density: 1.5–2.5). Table 3 presents geometric and surface cover properties for each LCZ.

Limitations

Some limitations of this study should be discussed. First, the integrated modeling approach does not consider local-scale advection or vertical mixing at the boundary-layer scale, and it is acknowledged that ENVI-met may have additional limitations in accurately simulating vertical mixing within the urban canopy layer⁶⁷. Second, this study assumed that the building construction is the same across all cities, using the standard LCZ scheme. It is warranted to take a more precise modeling approach of realistic urban environments and buildings in future studies. Future works should incorporate the large-scale and long-term experimental data to gain a better understanding of the holistic potential of green and cool roofs under different ambient environments. Future studies are also warranted to compare the energy-saving effects of green roofs and cool roofs with detailed divisions, such as extensive/intensive green roofs, and cool roofs composed of different materials. Simulations should be carried out with increased flexibility in model settings and empirical parameters. By incorporating a broader range of geographic locations, building conditions, and climate variations, more specific knowledge can be offered to global users.

Reporting summary

Further information on research design is available in the Nature Research Reporting Summary linked to this article.

Data availability

The authors declare that the data supporting the findings of this study are available within the paper and its supplementary information files. Supplementary Note 4 includes the simulated data for scenario analysis, while Supplementary Note 5 includes the simulated data for future energy-saving projections.

Received: 23 May 2023; Accepted: 23 March 2024; Published online: 03 April 2024

References

1. Mahtta, R. et al. Urban land expansion: the role of population and economic growth for 300+ cities. *Npj Urban Sustain.* **2**, 5 (2022).
2. Joosse, S., Hensle, L., Boonstra, W. J., Ponzelar, C. & Olsson, J. Fishing in the city for food—a paradigmatic case of sustainability in urban blue space. *npj Urban Sustain.* **1**, 41 (2021).
3. Yang, J., Xin, J., Zhang, Y., Xiao, X. & Xia, J. C. Contributions of sea-land breeze and local climate zones to daytime and nighttime heat island intensity. *npj Urban Sustain.* **2**, 12 (2022).
4. Aram, F., Higuera Garcia, E., Solgi, E. & Mansournia, S. Urban green space cooling effect in cities. *Heliyon* **5**, e01339 (2019).
5. Reyna, J. L. & Chester, M. V. Energy efficiency to reduce residential electricity and natural gas use under climate change. *Nat. Commun.* **8**, 14916 (2017).
6. Howard, L. *The Climate of London*, Vol. 3 (Harvey and Darton, J. and A. Arch, Longman, Hatchard, S. Highley [and] R. Hunter, 1833).
7. Oke, T. R. The energetic basis of the urban heat island. *Q. J. R. Meteorol. Soc.* **108**, 1–24 (1982).
8. Estrada, F., Botzen, W. J. W. & Tol, R. S. J. A global economic assessment of city policies to reduce climate change impacts. *Nat. Clim. Change.* **7**, 403–406 (2017).
9. Nejat, P., Jomehzadeh, F., Taheri, M. M., Gohari, M. & Majid, M. Z. A. A global review of energy consumption, CO2 emissions and policy in the

- residential sector (with an overview of the top ten CO₂ emitting countries). *Renew. Sustain. Energy Rev.* **43**, 843–862 (2015).
10. International Energy Agency. Directorate of Sustainable Energy Policy. *Transition to Sustainable Buildings: Strategies and Opportunities to 2050* (ed Organization for Economic Co-operation and Development) (OECD, 2013).
 11. Kontokosta, C. E., Spiegel-Feld, D. & Papadopoulos, S. The impact of mandatory energy audits on building energy use. *Nat. Energy* **5**, 309–316 (2020).
 12. Zhou, N., Khanna, N., Feng, W., Ke, J. & Levine, M. Scenarios of energy efficiency and CO₂ emissions reduction potential in the buildings sector in China to year 2050. *Nat. Energy* **3**, 978–984 (2018).
 13. Costanzo, V., Evola, G. & Marletta, L. Energy savings in buildings or UHI mitigation? Comparison between green roofs and cool roofs. *Energy Build.* **114**, 247–255 (2016).
 14. Santamouris, M. Cooling the cities—a review of reflective and green roof mitigation technologies to fight heat island and improve comfort in urban environments. *Sol. Energy* **103**, 682–703 (2014).
 15. Zheng, Y. & Weng, Q. Modeling the effect of green roof systems and photovoltaic panels for building energy savings to mitigate climate change. *Remote Sens.* **12**, 2402 (2020).
 16. Niachou, K. P. A., Santamouris, M., Tsangrassoulis, A. & Mihalakakou, G. Analysis of the green roof thermal properties and investigation of its energy performance. *Energy Build.* **33**, 719–729 (2001).
 17. Castleton, H. F., Stovin, V., Beck, S. B. M. & Davison, J. B. Green roofs; building energy savings and the potential for retrofit. *Energy Build.* **42**, 1582–1591 (2010).
 18. Romeo, C. & Zinzi, M. Impact of a cool roof application on the energy and comfort performance in an existing non-residential building. A Sicilian case study. *Energy Build.* **67**, 647–657 (2013).
 19. He, Y., Yu, H., Ozaki, A. & Dong, N. Thermal and energy performance of green roof and cool roof: a comparison study in Shanghai area. *J. Clean. Prod.* **267**, 122205 (2020).
 20. Li, X. et al. Urban heat island impacts on building energy consumption: a review of approaches and findings. *Energy* **174**, 407–419 (2019).
 21. Wong, N. H. et al. Evaluation of the impact of the surrounding urban morphology on building energy consumption. *Sol. Energy* **85**, 57–71 (2011).
 22. Yu, C. & Hien, W. N. Thermal benefits of city parks. *Energy Build.* **38**, 105–120 (2006).
 23. Hosseini, M., Bigtashi, A. & Lee, B. A systematic approach in constructing typical meteorological year weather files using machine learning. *Energy Build.* **226**, 110375 (2020).
 24. Chan, A. L. S. & Chow, T. T. Energy and economic performance of green roof system under future climatic conditions in Hong Kong. *Energy Build.* **64**, 182–198 (2013).
 25. Hall, I., Prairie, R., Anderson, H. & Boes, E. *Generation of a Typical Meteorological Year for 26 SOLMET Stations* (Sandia Labs., Albuquerque, NM, USA, 1978).
 26. Fumo, N. A review on the basics of building energy estimation. *Renew. Sustain. Energy Rev.* **31**, 53–60 (2014).
 27. Beck, H. E. et al. Present and future Koppen-Geiger climate classification maps at 1-km resolution. *Sci Data* **5**, 180214 (2018).
 28. Yazdani, H. & Baneshi, M. Building energy comparison for dynamic cool roofs and green roofs under various climates. *Sol. Energy* **230**, 764–778 (2021).
 29. Zinzi, M. & Agnoli, S. Cool and green roofs. An energy and comfort comparison between passive cooling and mitigation urban heat island techniques for residential buildings in the Mediterranean region. *Energy Build.* **55**, 66–76 (2012).
 30. Stewart, I. D. & Oke, T. R. Local climate zones for urban temperature studies. *Bull. Am. Meteorol. Soc.* **93**, 1879–1900 (2012).
 31. Bechtel, B. et al. Mapping local climate zones for a worldwide database of the form and function of cities. *ISPRS Int. J. Geo-inf.* **4**, 199–219 (2015).
 32. Patel, P., Kalyanam, R., He, L., Aliaga, D. & Niyogi, D. Deep learning-based urban morphology for city-scale environmental modeling. *PNAS Nexus* **2**, pgad027 (2023).
 33. Das, M. & Das, A. Assessing the relationship between local climatic zones (LCZs) and land surface temperature (LST)—a case study of Sriniketan-Santiniketan Planning Area (SSPA), West Bengal, India. *Urban Clim.* **32**, 100591 (2020).
 34. Yang, J. et al. Understanding land surface temperature impact factors based on local climate zones. *Sustain. Cities Soc.* **69**, 102818 (2021).
 35. Yang, J., Xin, J., Zhang, Y., Xiao, X. & Xia, J. C. Contributions of sea-land breeze and local climate zones to daytime and nighttime heat island intensity. *npj Urban Sustain.* **2**, 12 (2022).
 36. Yang, J. et al. Green and cool roofs' urban heat island mitigation potential in tropical climate. *Sol. Energy* **173**, 597–609 (2018).
 37. Silva, C. M., Gomes, M. G. & Silva, M. Green roofs energy performance in Mediterranean climate. *Energy Build.* **116**, 318–325 (2016).
 38. Wong, N. H., Tan, C. L., Kolokotsa, D. D. & Takebayashi, H. Greenery as a mitigation and adaptation strategy to urban heat. *Nat. Rev. Earth Environ.* **2**, 166–181 (2021).
 39. Heusinger, J., Sailor, D. J. & Weber, S. Modeling the reduction of urban excess heat by green roofs with respect to different irrigation scenarios. *Build. Environ.* **131**, 174–183 (2018).
 40. Meng, L. et al. Artificial light at night: an underappreciated effect on phenology of deciduous woody plants. *PNAS Nexus* **1**, pgac046 (2022).
 41. Hamel, P. et al. Mapping the benefits of nature in cities with the INVEST software. *npj Urban Sustain.* **1**, 25 (2021).
 42. Wang, W. et al. Benchmarking urban local weather with long-term monitoring compared with weather datasets from climate station and EnergyPlus weather (EPW) data. *Energy Rep.* **7**, 6501–6514 (2021).
 43. Renné, D. Resource assessment and site selection for solar heating and cooling systems. In *Advances in Solar Heating and Cooling*, 13–41 (Elsevier, 2016).
 44. Shen, P. Impacts of climate change on U.S. building energy use by using downscaled hourly future weather data. *Energy Build.* **134**, 61–70 (2017).
 45. Randall, D. A. et al. Climate models and their evaluation. in *Climate Change 2007: The Physical Science Basis. Contribution of Working Group I to the Fourth Assessment Report of the IPCC (FAR)*, 589–662 (Cambridge University Press, 2007).
 46. Williams, K. D. et al. The Met Office Global Coupled Model 3.0 and 3.1 (GC3.0 and GC3.1) Configurations. *J. Adv. Model. Earth Syst.* **10**, 357–380 (2018).
 47. Tatebe, H. et al. Description and basic evaluation of simulated mean state, internal variability, and climate sensitivity in MIROC6. *Geosci. Model Dev.* **12**, 2727–2765 (2019).
 48. Yukimoto, S. et al. The Meteorological Research Institute Earth System Model version 2.0, MRI-ESM2.0: description and basic evaluation of the physical component. *J. Meteorol. Soc. Jpn. Ser. II* **97**, 931–965 (2019).
 49. Lovato, T. et al. CMIP6 simulations with the CMCC Earth system model (CMCC-ESM2). *J. Adv. Model. Earth Syst.* **14**, e2021MS002814 (2022).
 50. Bi, D. et al. Configuration and spin-up of ACCESS-CM2, the new generation Australian community climate and earth system simulator coupled model. *J. South. Hemisph. Earth Syst. Sci.* **70**, 225–251 (2020).
 51. Wu, T. et al. BCC-CSM2-HR: a high-resolution version of the Beijing Climate Center Climate System Model. *Geosci. Model Dev.* **14**, 2977–3006 (2021).
 52. Pierce, D. W., Barnett, T. P., Santer, B. D. & Gleckler, P. J. Selecting global climate models for regional climate change studies. *Proc. Natl. Acad. Sci.* **106**, 8441–8446 (2009).
 53. IPCC, Climate change 2021: the physical science basis. *Contribution of Working Group I to the Sixth Assessment Report of the*

- Intergovernmental Panel on Climate Change* (Cambridge University Press, 2021).
54. IPCC, Climate change 2013: the physical science basis. *Contribution of Working Group I to the Fifth Assessment Report of the Intergovernmental Panel on Climate Change* (Cambridge University Press, 2013).
 55. Riahi, K. et al. The Shared Socioeconomic Pathways and their energy, land use, and greenhouse gas emissions implications: an overview. *Glob. Environ. Change*. **42**, 153–168 (2017).
 56. Olivieri, F., Di Perna, C., D'Orazio, M., Olivieri, L. & Neila, J. Experimental measurements and numerical model for the summer performance assessment of extensive green roofs in a Mediterranean coastal climate. *Energy Build.* **63**, 1–14 (2013).
 57. Miller, C. The building data genome project 2, energy meter data from the ASHRAE great energy predictor III competition. *Sci. Data*. **7**, 368 (2020).
 58. Bamdad, K., Cholette, M. E., Omrani, S. & Bell, J. Future energy-optimised buildings—Addressing the impact of climate change on buildings. *Energy Build.* **231**, 110610 (2021).
 59. Belcher, S. E., Hacker, J. N. & Powell, D. S. Constructing design weather data for future climates. *Build. Serv. Eng. Res. Technol.* **26**, 49–61 (2005).
 60. Crawley, D. B. et al. EnergyPlus: creating a new-generation building energy simulation program. *Energy Build.* **33**, 319–331 (2001).
 61. Morakinyo, T. E., Dahanayake, K. W. D. K. C., Ng, E. & Chow, C. L. Temperature and cooling demand reduction by green-roof types in different climates and urban densities: A co-simulation parametric study. *Energy Build.* **145**, 226–237 (2017).
 62. Bruse, M. & Fleer, H. Simulating surface–plant–air interactions inside urban environments with a three dimensional numerical model. *Environ. Model. Softw.* **13**, 373–384 (1998).
 63. Huttner, S. *Further Development and Application of the 3d Microclimate Simulation ENVI-Met*. Dissertation. Johannes Gutenberg-Universität in Mainz, Vol. 147 (2012).
 64. Tsoka, S., Tsikaloudaki, A. & Theodosiou, T. Analyzing the ENVI-met microclimate model's performance and assessing cool materials and urban vegetation applications—a review. *Sustain. Cities Soc.* **43**, 55–76 (2018).
 65. Demuzere, M. et al. A global map of local climate zones to support earth system modelling and urban-scale environmental science. *Earth Syst. Sci. Data* **14**, 3835–3873 (2022).
 66. Zheng, Y. et al. GIS-based mapping of Local Climate Zone in the high-density city of Hong Kong. *Urban Clim.* **24**, 419–448 (2018).
 67. Krähenhoff, E. S. et al. Cooling hot cities: a systematic and critical review of the numerical modelling literature. *Environ. Res. Lett.* **16**, 053007 (2021).

Acknowledgements

This work was supported by the Research Talent Hub of the Innovation and Technology Fund and the Global STEM Professorship of Hong Kong Special Administrative Region Government.

Author contributions

Siqi Jia took charge of conceptualization, methodology development, software implementation, validation, formal analysis, investigation, resource management, data curation, and drafting the original manuscript. Qihao Weng directed the study and contributed to the conceptualization, reviewing and editing of the manuscript, and project administration. Cheolhee Yoo was involved in the methodology development and investigation. Huijuan Xiao and Qingwei Zhong contributed to the methodology development and assisted in reviewing and editing the manuscript.

Competing interests

The authors declare no competing interests.

Additional information

Supplementary information The online version contains supplementary material available at <https://doi.org/10.1038/s42949-024-00159-8>.

Correspondence and requests for materials should be addressed to Qihao Weng.

Reprints and permissions information is available at <http://www.nature.com/reprints>

Publisher's note Springer Nature remains neutral with regard to jurisdictional claims in published maps and institutional affiliations.

Open Access This article is licensed under a Creative Commons Attribution 4.0 International License, which permits use, sharing, adaptation, distribution and reproduction in any medium or format, as long as you give appropriate credit to the original author(s) and the source, provide a link to the Creative Commons licence, and indicate if changes were made. The images or other third party material in this article are included in the article's Creative Commons licence, unless indicated otherwise in a credit line to the material. If material is not included in the article's Creative Commons licence and your intended use is not permitted by statutory regulation or exceeds the permitted use, you will need to obtain permission directly from the copyright holder. To view a copy of this licence, visit <http://creativecommons.org/licenses/by/4.0/>.

© The Author(s) 2024